Radicals and Anions of Siloles and Germoles

Crispin R. W. Reinhold,[a] Marc Schmidtmann,[a] Boris Tumanskii,*[b] and Thomas Müller*[a]

In memory of Zvi Rappoport

Abstract: The synthesis of persistent sila- and germacyclopentadienyl (silolyl- and germolyl-) radicals by careful stoichiometric reduction of the corresponding halides with potassium is reported. The radicals were characterized by EPR spectroscopy and trapping reactions. The reduction of *tris*(trimethylsilyl)silyl-substituted halides was successful while smaller substituents (i.e., *t*-Butyl, Ph) gave the corresponding dimers. The EPR spectroscopic parameter of the synthesized tetrolyl radicals indicate only small spin delocalization to the butadiene unit due to cross-hyperconjugation. Silolyl- and germolyl anions are unavoidable byproducts and are isolated in the form of their potassium salts and characterized by X-ray crystallography. The comparison of the molecular structures of two closely related potassium silolides provided an example for different coordination of the potassium cation to the silolyl anion (η^1 vs. η^5 coordination) that triggers the switch between delocalized and localized states.

Introduction

Progress in the chemistry of tetroles **I**, the heavier analogs of cyclopentadiene, is driven by the favorable photophysical properties of these compounds (Figure 1).[1–4] The cross-hyperconjugation between the butadiene part and the tetrylene unit lowers their absorption energy and promotes their application in optoelectronic devices.[5–8] The discovery of the aggregation induced emission effect in perarylated siloles additionally fueled the interest in this class of compounds.[9–12] The second mainspring for the development of the chemistry of tetroles was the possible occurrence of aromaticity in the negatively charged ions, **II** and **III**, and their applications as ligands in transition metal chemistry.[13–16] During the last years, the group of Saito and the Oldenburg team contributed to this field by demonstrating that tetrole dianions **III** are suitable precursors for a wide variety of novel compounds with the tetrel element in unusual coordination environments.[13,16–19] In view of the vast existing body of knowledge on tetrole's material chemistry, we asked ourselves if the favorable photophysical properties of tetroles might be combined with magnetic properties resulting from an unpaired spin as for example in tetrolyl radicals **IV**. An inspiration came from one report by the West group who communicated on the existence and stability of a silolyl-based biradical **V** with triplet ground state and its surprisingly low reactivity.[20] We report here on the successful preparation of neutral silolyl and germolyl radicals **IV** (E=Si, Ge) and some of their properties. In addition, we report on a structural study on closely related tetrolyl anions **II** (E=Si, Ge) and their transformation between delocalized and localized states induced by substituent effects.

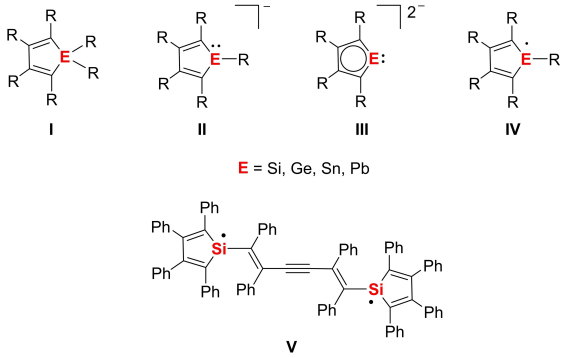

Figure 1. Tetroles, tetrolyl anions, dianions and radicals and the persistent disilolyldiradical reported by Toulokhonova et al.[20]

Results and Discussion

We attempted the synthesis of germolyl radicals by careful stoichiometric reduction of the corresponding germolyl halides **1** with potassium graphite according to procedures published by the group of Sekiguchi.[21–23] In the case of 1-phenyl and 1-*tert*-butyl substituted germolyl halides **1a** and **1b** only the

[a] *Dr. C. R. W. Reinhold, Dr. M. Schmidtmann, Prof. Dr. T. Müller*
Institute of Chemistry
Carl von Ossietzky University Oldenburg
Carl von Ossietzky-Str. 9–11, 26129 Oldenburg (Germany, European Union)
E-mail: thomas.mueller@uni-oldenburg.de

[b] *Dr. B. Tumanskii*
Schulich Faculty of Chemistry
Technion-Israel Institute of Technology
Haifa, 32000 (Israel)
E-mail: tboris@technion.ac.il

Supporting information for this article is available on the WWW under https://doi.org/10.1002/chem.202101415

corresponding Ge–Ge bonded dimers **2a,b** were obtained, indicating insufficient steric shielding of the intermediate germolyl radical. Both compounds were isolated in moderate to good yields and fully characterized by NMR spectroscopy and their molecular structures in the solid state were determined by X-ray diffraction (XRD) analysis. Increasing the size of the substituent R at the germanium atom from the *tert*-butyl to the *tris*(trimethylsilyl)silyl group finally allowed the detection of the germolyl radical **3c** in high concentrations by EPR spectroscopy after reduction of germolyl chloride **1c** (Scheme 1).[24] The trapping reaction with cyclohexadiene gives *1H*-germole **4** in high yield. The identity of germole **4** was verified by independent synthesis from germole chloride **1c** (Scheme 2).

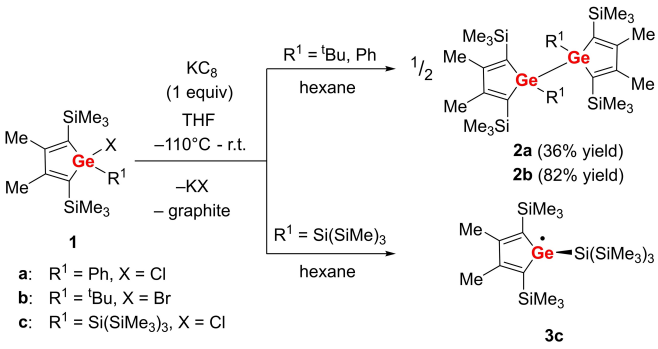

Scheme 1. Synthesis of *bis*-germoles **2** and of germolyl radical **3**.

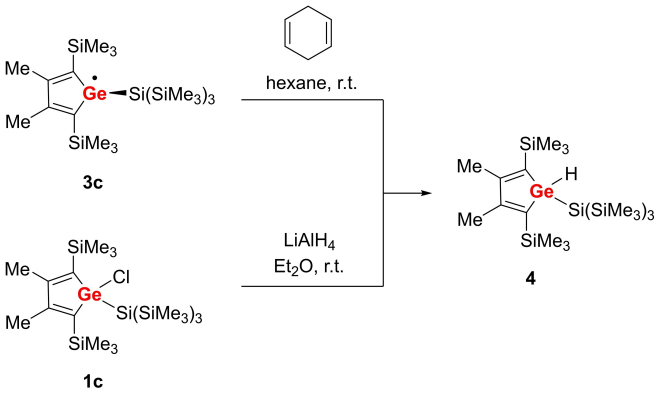

Scheme 2. Trapping of germolyl radical **3c** and independent synthesis of *1H*-germole **4**.

Table 1. Cone angles Θ [°] for the substituents R^1 along with calculated bond dissociation energies (BDE [kJ mol^{-1}]) and Ge–Ge bond lengths *d* of *bis*-germoles **2** [pm] and calculated substituent effect of the substituent R^1 on the stability of germolyl radicals **3** (ΔE [kJ mol^{-1}]) (at M06-2X/6-311+G(d,p), data for hexamethyl digermane is given in the right column and experimental data in parenthesis).

R^1	H	Ph	tBu	$SiMe_3$	$Si(SiMe_3)_3$	$(Me_3Ge)_2$
Θ[a]	-	135	137	126	185	–
d	247	249 (246.0)[b]	251 (248.4)[b]	247	265	245 (241.6)[c]
BDE	277	280	267	271	96	273 (282 ± 15)[d]
ΔE	0	+7	+1	−11	−17	–

[a] Ref [25]. [b] This work. [c] Ref. [26] [d] Ref. [27].

The results of density functional calculations guided our choice of the substituent R^1 of the starting germolyl halides (Table 1).[28] The spatial requirements of the phenyl and the *tert*-butyl substituent are very similar as shown by their almost identical cone angles Θ.[25] As a result, their influence on the formation of a Ge–Ge linkage is the same. The Ge–Ge atomic distances in *bis*-germoles **2a**, **b** are almost identical and the calculated bond dissociation energies (BDEs) are very similar. In contrast, the steric effect of the *tris*(trimethylsilyl)silyl group as measured by its cone angle Θ is substantially larger. The results of the computation predicted a significant increase of the Ge–Ge bond length of the dimer **2c** and a considerable weakening of the Ge–Ge bond (Table 1). In addition, the *tris*(trimethylsilyl)silyl substituent stabilizes the germolyl radical compared to the hydrogen substituted germolyl radical (ΔE < 0, see Table 1 and Supporting Information material for details).[29] Both factors favored the formation of the germolyl radical **3c**. The comparison with the data calculated for the trimethylsilyl substituent, which also stabilizes the silolyl radical, suggests that the steric factors are however decisive. These results can be transferred to siloles, the *tris*(trimethylsilyl)silyl substituent allowed the synthesis of the corresponding silolyl radical by reduction of silolyl chloride **5** (Scheme 3).[24]

The reduction of germolyl chloride **1c** and silolyl chloride **5** were performed at low temperature in THF and after changing to a non-polar solvent such as hexane intensive EPR signals of the neutral radicals **3c** and **6** were detected. In the absence of air and moisture, the germolyl radical **3c** is stable in solution for weeks. In contrast, the silolyl radical is persistent but decomposed over several days. In both cases, we were not able to grow crystals suitable for XRD analysis. The EPR data for both radicals are summarized in Table 2 and the spectrum of silolyl radical **6** is shown in Figure 2 along with its simulation applying the measured parameters. We refer to the Supporting Information for more detailed spectroscopic information. G-value and hyperfine couplings *a* for both radicals are close to related persistent neutral silyl- or germyl radicals (Figure 3) and the spectroscopic data agrees with the suggested molecular structure.[30–31] Particular informative are the hyperfine coupling constants (hfcc) $a(E^{\alpha})$ of the group 14 element with the unpaired electron (decet with $a = 2.7$ mT for germolyl radical **3c** and duplet of $a = 6.1$ mT for silolyl radical **6**). Their analysis allows a tentative discussion of its coordination environment. Relatively large hyperfine couplings are detected for pyramidal radicals such as **8** and **9**, due to the larger contribution of s-type atomic orbitals of the group 14 element to the SOMO

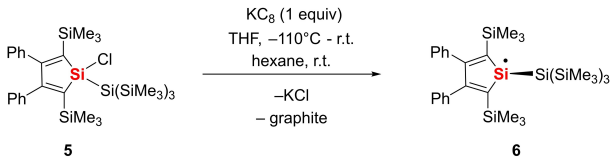

Scheme 3. Synthesis of silolyl radical **6**.

Table 2. Experimental ESR parameters (g-value, hyperfine coupling constant *a*, hexane, r.t.) and calculated hyperfine a^{calc} for radicals **3c** and **6** and for model compounds **7**.

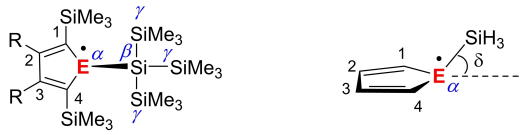

3c: E = Ge R = Me **7a:** E = Ge
6: E = Si R = Ph **7b:** E = Si

cpd	G	a [mT]	a^{calc} [mT]
3c	2.018 g_{11} = 2.031[a] g_{22} = 2.026[a] g_{33} = 1.997[a]	2.7 (^{73}Ge$^{\alpha}$) 1.7 (^{29}Si$^{\beta}$) 0.8 (^{29}Si$^{\gamma}$) 3.0 (^{13}C) 2.3 (^{13}C)	2.6 (^{73}Ge$^{\alpha}$)[b]
6	2.004	6.1 (^{29}Si$^{\alpha}$) 0.8 (^{29}Si$^{\gamma}$)[c] 1.4 (^{13}C) 0.02 (^{1}H)	6.5 (^{29}Si$^{\alpha}$)[b]
7a[d]			δ = 0°, 1.9 (^{73}Ge$^{\alpha}$) δ = 85°, 9.1 (^{73}Ge$^{\alpha}$)
7b[d]			δ = 0°, 2.9 (^{29}Si$^{\alpha}$) δ = 85°, 22.9 (^{29}Si$^{\alpha}$)

[a] At 103 K in frozen hexane. [b] Calculated at PBEO/Def2-TZVPD//M06-2X/Def2-TZVP. [c] Calculated at M06-2X/6-311+G(d,p). [c] The assignment is based on the high intensity of the satellite signals (3 Si_{γ}). A signal for the hfc to Si_{α} was not detected (see Supporting Information material for further information). [d] Calculated at M06-2X/6-311+G(d,p). The tilt angle δ is defined by the line between the midpoint of the C2–C3 bond and the element atom E and by the E–Si vector.

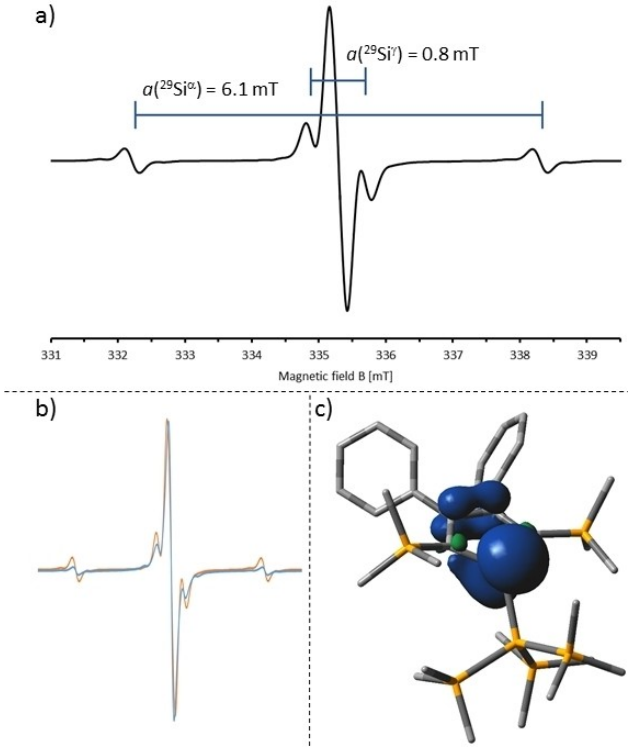

Figure 2. a) EPR spectrum of 1-*tris*(trimethylsilyl)silylsilolyl radical **6** in hexane solution at room temperature; 9403.0 MHz; Mod.-Ampl. = 0.075 mT; MW-Att. = 3.0 dB. b) Simulated EPR spectrum of radical **6** (blue experimental, orange simulated). c) Calculated spin density of radical **6** at isovalue = 0.004 (PBE0/Def2-TZVPD//M06-2X/Def2-TZVP, hydrogen atoms are omitted for clarity.

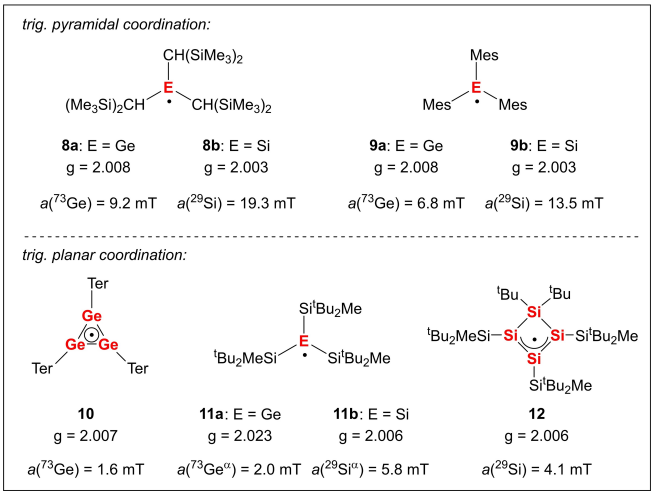

Figure 3. EPR parameters of stable neutral germyl and silyl radicals.

(Figure 3).[31–35] The group 14 element adopts a trigonal planar coordination environment in radicals **10–12** according to XRD investigations and the SOMO has almost pure p-character.[36–41] Consequently, the hyperfine coupling to the silicon or germanium atom is significantly smaller (Figure 3). Before this background, the relatively large hyperfine coupling $a(E^{\alpha})$ for the heterolyl radicals **3c** and **6** suggest a pyramidal coordination of the tetrel element. In agreement, the results of DFT calculations for the model heterolyl radicals **7** show that $a(E^{\alpha})$ varies significantly with the degree of pyramidalization at the tetrel element E (i.e. for E=Ge from 1.9 mT for a trigonal planar coordination up to a maximum of 8.9 mT, see Table 2).[28] Full structure optimization at the M06-2X/Def2-TZVP level result in pyramidal structures for radicals **3c** (δ = 37°; $\Sigma\alpha$(Ge) = 340°) and **6** (δ = 35°; $\Sigma\alpha$(Si) = 345°). For both optimized molecular structures hyperfine coupling constants close to the experimental values are calculated (Table 2). The shape of the calculated surface diagrams of the SOMO indicate predominant localization of the unpaired electron at the tetrel atom with delocalization tails at the carbon atoms C2 and C3 (see Figure 2c, for an example). This suggests interaction between the π^* orbital of the butadiene part and the singly occupied orbital at the tetrel element, which is reminiscent to the π^*-σ^* cross hyperconjugation in the closed shell heteroles.[5,7] The here derived localized electronic structure of heterolyl radicals **3c** and **6** agrees with the calculated structural parameters which indicate a localized heterocyclopentadiene structure for both radicals comparable to that of the precursor chlorides **1c** and **5** or the bisgermoles **2** (Table 3).

In several runs, we isolated from hexane solutions of the reduction of germole chloride **1c** crystals of the potassium germolide K[**13**]. K[**13**] was independently synthesized by reduction of chloride **1c** with two equivalents of KC_8 in THF in

Table 3. Structural parameters of heterolyl radicals and anions (from XRD analysis, calculated parameters for radicals and for free anions are given in italics).

cpd	E	C^1–C^2/ C^3–C^4 [pm]	C^2–C^3 [pm]	Δ [pm][a]	E–C [pm]	Σα(E) [°][d]
1c[b]	Ge	135.8	150.9	15.1	195.8	323.1[e]
5[b]	Si	136.4	151.4	15.0	187.1	324.4[e]
2a	Ge	135.5	150.3	14.8	195.7	313.1
2b	Ge	135.7	150.0	14.3	196.6	308.3
3c[c]	Ge	*135.8*	*149.4*	*13.6*	*195.2*	*340.4*
6[c]	Si	*137.1*	*148.2*	*11.1*	*184.3*	*344.8*
K[**13**]	Ge	137.8	147.1	9.3	200.4	292.6
K[**13**] (THF)	Ge	137.1	145.5	8.4	200.7	289.7
[**13**]$^{-}$ [c]	Ge	*137.2*	*147.8*	*10.6*	*201.2*	*288.9*
K[**14**] (C_6H_6)	Si	139.5	145.0	5.5	188.0	314.9
[**14**]$^{-}$ [c]	Si	*139.0*	*145.0*	*6.0*	*186.8*	*307.3*
K[**14**] (η^5)[c]	Si	*143.0*	*141.7*	*−1.3*	*181.6*	*357.7*
K[**14**] (η^1)[c]	Si	*137.5*	*146.9*	*9.4*	*188.6*	*307.9*
K[**16**] 2THF	Si	143.6	141.5	−2.1	182.0	358.1

[a] Δ: difference between C^2–C^3 and the mean value of C^1–C^2 and C^3–C^4. [b] From ref. [24] [c] Calculated at M06-2X/6-311+G(d,p). [d] Sum of the bond angles around the tetrel element E. [e] Measured as sum of the bond angles involving carbon and silicon atoms and the tetrel element E.

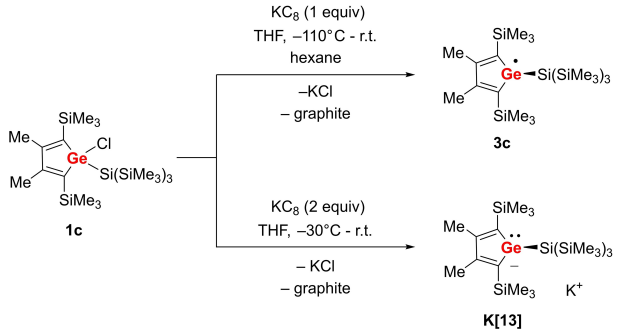

Scheme 4. Products of the reduction of germolyl chloride **3c** with potassium graphite, KC_8.

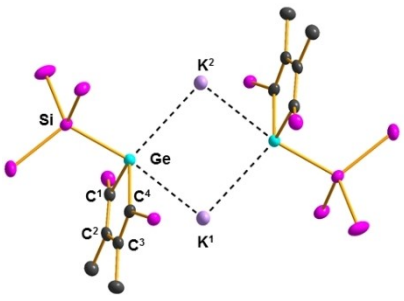

Figure 4. Structure of the coordination dimer of K[**13**] in the crystal. (representation as thermal ellipsoid at 50% probability, hydrogen atoms are omitted, the alkyl groups at all silicon atoms are not shown, color code: black C, pink Si, turquoise Ge, violet K, red O). Selected structural parameters [pm]: K^1 - Ge 327, K^2 - Ge 350, K^1 - C^1 = 319, K^1 - C^2 = 321, K^1 - C^1 = 32, K^1 - C^1 = 326, δ = 72°. For additional relevant structural parameters, see Table 3.

49% isolated yield (Scheme 4). It was characterized by NMR spectroscopy and by XRD analysis of suitable crystals of K[**13**] and of its THF solvate. The isolation of the potassium germolide K[**13**] suggested to us that radical **3c** might be formed by a comproportionation reaction between germolyl chloride **1c** and the germolide [**13**]$^{-}$, after over-reduction of the chloride by KC_8. Similarly, the potassium silolide K[**14**] was isolated in small quantities from the reaction mixtures of the reduction of silolyl chloride **5** with KC_8 and its solid state structure was solved.

The dominating structural motif in the solid state structures of potassium germolide K[**13**] and of its THF solvate are dimers in which two germolide anions are connected via two η^1/η^5-coordinated potassium cations (Figure 4). The potassium silolide K[**14**] forms a one-dimensional coordination polymer, in which the individual silole anions are connected via potassium cations that are η^1-coordinated to the tricoordinated silicon atom and to the phenyl substituents in 3,4 position (Figure 5a). Like previous examples of 1-*tris*(trimethylsilyl)silyl-substituted germole and silole anions reported by the Tilley group,[42–43] anions [**13**]$^{-}$ and [**14**]$^{-}$ show a trigonal pyramidal coordination around the tetrel atom and a localized ring structure with strongly alternating C=C double and C–C single bonds as shown by the bond length difference Δ (Table 3).[44] These structural features are strong and conclusive arguments for the non-aromaticity of silole and germole anions.

There is however clear evidence that coordination of metal cations to the heterole anion do influence the structure of the five-membered ring and that a switch between delocalized aromatic and localized non-aromatic structures can be triggered by the counter cation. The Tilley group reported germolyl- and silolyl complexes of transition metal ions such as Hf(IV), Fe(II) and Ru(II) with η^5-coordinated heterolyl anions.[45–49] Kovacs and coworkers recently reported the structure of a contact ion pair between lithium cation and a silolyl anion with a delocalized

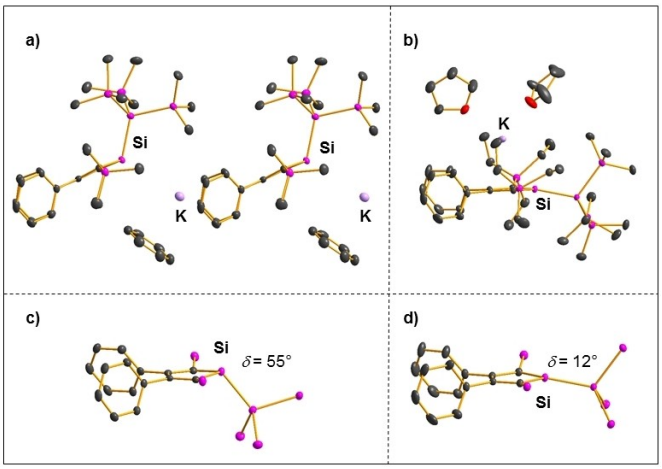

Figure 5. a) Part of the polymeric structure of K[**14**]•(C_6H_6) in the crystal. b) Structure of the ion pair of K[**16**] •2THF. c) Molecular structure of silolyl anion [**14**]$^{-}$ in the crystal. d) Molecular structure of silolyl anion [**16**]$^{-}$ in the crystal (representation as thermal ellipsoid at 50% probability, hydrogen atoms are omitted, in c and d also the alkyl groups at all silicon atoms are not shown, color code: black C, pink Si, violet K, red O). For relevant structural parameters, see Table 3.

aromatic structure.[50] Lee and colleagues gave evidence for similar phenomena in the case of disilagermolyl anion and trisilagermolyl anions.[51–52] Finally, we showed that potassium salts from germolyl anions switch from delocalized aromatic to localized non-aromatic states triggered by the complexation of the potassium ion.[53]

Before this background, we tested computationally several structures of the ion pair K[**14**] and found that η^5 coordination of the potassium cation is preferred by 38 kJ mol^{-1} over the corresponding η^1-structure (Figure 6). In the η^5-structure the coordination environment of the silicon atom is almost ideal trigonal planar, and the CC atomic distances are almost equal ($\Delta = -1.3$ pm, Table 3). These structural details hint to electron delocalization in the five-membered ring. Nucleus independent chemical shift (NICS) calculations support the higher degree of aromaticity for the η^5-structure of K[**14**] (Figure 6).[54–55] Nevertheless, in the polymeric structure of K[**14**](C_6H_6) the η^1 coordination of the potassium cation by the silicon atom is favored (Figure 5a,c). Since we were not successful to crystallize the delocalized η^5-coordinated variant of K[**14**], we tested small variations of the silyl groups in 1,4 position of the silolyl anion. Reduction of triethylsilyl-substituted silole chloride **15** with potassium graphite in THF gave K[**16**] as THF solvate (Scheme 5). Its molecular structure in the crystal is shown in Figure 5b,d and pertinent structural parameters are given in Table 3. The potassium cation is η^5-coordinated and the silolyl ring adopts a delocalized structure as shown by almost equalized inner cyclic CC bonds ($\Delta = -2.1$ pm), short Si–C bonds and an almost trigonal planar coordination environment for the silicon atom (see Table 3). The pair of potassium silolides K[**14**] and K[**16**] are an additional example, which shows that subtle changes in the constitution (different remote substituents $SiEt_3$ vs. $SiMe_3$) and/or solvent (THF solvate vs. benzene solvate) forces different coordination between heterolyl anion and counter cation in the solid state that are accompanied by a significant change of the degree of delocalization in the heterole ring.

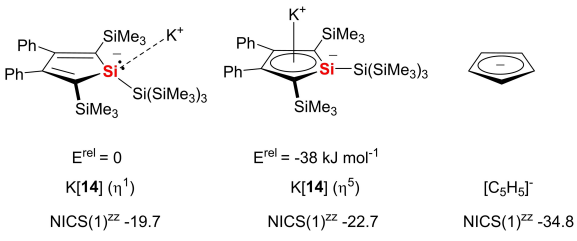

Figure 6. Relative energies E^{rel} of computed gas phase structures of the ion pair K[**14**] with different coordination environments and the calculated NICS(1)^{zz} parameter (Banquo atom 100 pm below the plane of the five-membered ring, only the tensor component orthogonal to the ring plane is given). The data for cyclopentadienide is shown for comparison (M06-2X/6-311 + G(d,p)). Selected structural parameters [pm]: η^1: K–Si 317.8, η^5: K–Si 317.7. For additional relevant structural parameters, see Table 3.

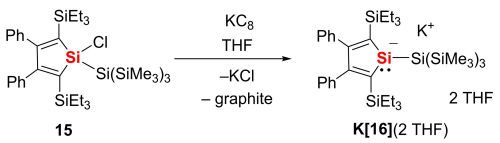

Scheme 5. Synthesis of potassium silolide THF solvate K[**16**] •2THF).

Conclusion

Neutral silolyl and germolyl radicals were prepared by reduction of the corresponding chlorides and were characterized by ESR spectroscopy supported by the results of quantum mechanical calculations. Substituents at the radical centers as large as the *tris*(trimethylsilyl)silyl group are needed to prevent dimerization to the corresponding ditetrelanes. The obtained radicals **3c** and **6** are persistent but reach by far not the stability reported for the *bis*-silolyl radical **V** by the West group. The analysis of the hyperfine coupling constant of the unpaired electron with the tetrel element indicates a pyramidalized structure of the heterolyl radicals with only little delocalization into the heterole ring. Our computational analysis suggests that the discernable spin delocalization in tetrolyl radicals **3c** and **6** is the result of cross hyperconjugation between the butadiene group and the tetrylenyl R-E$^{\cdot}$ unit.[7] *Tris*(trimethylsilyl)silyl-substituted heterolyl anions [**13**]$^-$ and [**14**]$^-$, which were isolated in the form of their potassium salts, are unavoidable byproducts of these reductions. Both anions show in the solid state the expected localized heterole structures with a trigonal pyramidal coordination environment of the germanium or silicon atom. Interestingly, the solid state structure of the closely related potassium silolide K[**16**] reveals a η^5-coordinated potassium ion, an almost trigonal planar coordination of the silole silicon atom and structural parameters of the silole ring that are typical for delocalized silolyl anions. Therefore, the pair K[**14**] and K[**16**] represent another example where the degree of delocalization in heterocyclopentadienyl anions is triggered by the coordination of the countercation.

Acknowledgements

This work was supported by the Deutsche Forschungsgemeinschaft (DFG-Mu1440/13-1, INST 184/108-1 FUGG). We thank Prof Y. Apeloig, Technion, Haifa, Israel for his support and hospitality during C.R.W.R.'s research internship in his laboratories. Open access funding enabled and organized by Projekt DEAL.

Conflict of Interest

The authors declare no conflict of interest.

Keywords: anions · conjugation · germanium · radical · silicon

[1] M. Shimizu, *Main Group Strategies towards Functional Hybrid Materials*, Eds.: T. Baumgartner, F. Jäckle, **2017**, pp. 163–195.
[2] S. Santra, *ChemistrySelect* **2020**, *5*, 9034–9058.
[3] Y. Cai, A. Qin, B. Z. Tang, *J. Mater. Chem. C* **2017**, *5*, 7375–7389.

[4] Y. Adachi, J. Ohshita, *Main Group Strategies towards Functional Hybrid Materials*, Eds.: T. Baumgartner, F. Jäckle, **2017**, pp. 237–267.
[5] S. Yamaguchi, K. Tamao, *Bull. Chem. Soc. Jpn.* **1996**, *69*, 2327–2334.
[6] S. Yamaguchi, T. Endo, M. Uchida, T. Izumizawa, K. Furukawa, K. Tamao, *Chem. Eur. J.* **2000**, *6*, 1683–1692.
[7] A. V. Denisova, J. Tibbelin, R. Emanuelsson, H. Ottosson, *Molecules* **2017**, *22*, 370.
[8] A. Pöcheim, G. A. Özpınar, T. Müller, J. Baumgartner, C. Marschner, *Chem. Eur. J.* **2020**, *26*, 17252–17260.
[9] J. Luo, Z. Xie, J. W. Y. Lam, L. Cheng, H. Chen, C. Qiu, H. S. Kwok, X. Zhan, Y. Liu, D. Zhu, B. Z. Tang, *Chem. Commun.* **2001**, 1740–1741.
[10] G. Yu, S. Yin, Y. Liu, J. Chen, X. Xu, X. Sun, D. Ma, X. Zhan, Q. Peng, Z. Shuai, B. Tang, D. Zhu, W. Fang, Y. Luo, *J. Am. Chem. Soc.* **2005**, *127*, 6335–6346.
[11] Z. Zhao, B. He, B. Z. Tang, *Chem. Sci.* **2015**, *6*, 5347–5365.
[12] J. L. Mullin, H. J. Tracy, *Aggregation-Induced Emission: Fundamentals and Applications, Volumes 1 and 2*, Eds.: A. Qin, B. Z. Tang, **2013**, pp. 39–60.
[13] M. Saito, M. Yoshioka, *Coord. Chem. Rev.* **2005**, *249*, 765–780.
[14] M. Saito, *Coord. Chem. Rev.* **2012**, *256*, 627–636.
[15] V. Y. Lee, A. Sekiguchi, *Angew. Chem. Int. Ed.* **2007**, *46*, 6596–6620, *Angew. Chem.* **2007**, *119*, 6716–6740.
[16] M. Saito, *Acc. Chem. Res.* **2018**, *51*, 160–169.
[17] Z. Dong, L. Albers, T. Müller, *Acc. Chem. Res.* **2020**, *53*, 532–543.
[18] L. Albers, P. Tholen, M. Schmidtmann, T. Müller, *Chem. Sci.* **2020**, *11*, 2982–2986.
[19] Z. Dong, J. M. Winkler, M. Schmidtmann, T. Müller, *Chem. Sci.* **2021**, *12*, 6287–6292.
[20] I. S. Toulokhonova, T. C. Stringfellow, S. A. Ivanov, A. Masunov, R. West, *J. Am. Chem. Soc.* **2003**, *125*, 5767–5773.
[21] T. Nozawa, M. Nagata, M. Ichinohe, A. Sekiguchi, *J. Am. Chem. Soc.* **2011**, *133*, 5773–5775.
[22] K. Taira, M. Ichinohe, A. Sekiguchi, *Chem. Eur. J.* **2014**, *20*, 9342–9348.
[23] T. Nozawa, M. Ichinohe, A. Sekiguchi, *Chem. Lett.* **2014**, *44*, 56–57.
[24] C. R. W. Reinhold, Z. Dong, J. M. Winkler, H. Steinert, M. Schmidtmann, T. Müller, *Chem. Eur. J.* **2018**, *24*, 848–854.
[25] A. Schulz, *Z. Anorg. Allg. Chem.* **2014**, *640*, 2183–2192.
[26] K. Aarset, E. M. Page, D. A. Rice, *J. Phys. Chem. A* **2010**, *114*, 7187–7190.
[27] R. Becerra, R. Walsh, *Phys. Chem. Chem. Phys.* **2019**, *21*, 988–1008.
[28] See the Supporting Information for details on the computations.
[29] C. H. Schiesser, S. Zahirovic, *J. Chem. Soc. Perkin Trans. 2* **1999**, 933–936.
[30] B. Tumanskii, M. Karni, Y. Apeloig, *Organosilicon Compounds*, Ed.: V. Y. Lee, Academic Press, **2017**, pp. 231–294.
[31] P. P. Power, *Chem. Rev.* **2003**, *103*, 789–810.
[32] A. Hudson, M. F. Lappert, P. W. Lednor, *J. Chem. Soc. Dalton Trans.* **1976**, 2369–2375.
[33] H. Sakurai, K. Mochida, M. Kira, *J. Organomet. Chem.* **1977**, *124*, 235–252.
[34] M. J. S. Gynane, M. F. Lappert, P. Riviere, M. Riviere-Baudet, *J. Organomet. Chem.* **1977**, *142*, C9-C11.
[35] C. Drost, J. Griebel, R. Kirmse, P. Lönnecke, J. Reinhold, *Angew. Chem. Int. Ed.* **2009**, *48*, 1962–1965; *Angew. Chem.* **2009**, *121*, 1996–1999.
[36] V. Y. Lee, A. Sekiguchi, *Eur. J. Inorg. Chem.* **2005**, *2005*, 1209–1222.
[37] A. Sekiguchi, T. Matsuno, M. Ichinohe, *J. Am. Chem. Soc.* **2001**, *123*, 12436–12437.
[38] A. Sekiguchi, T. Fukawa, M. Nakamoto, V. Y. Lee, M. Ichinohe, *J. Am. Chem. Soc.* **2002**, *124*, 9865–9869.
[39] A. Sekiguchi, T. Fukawa, V. Y. Lee, M. Nakamoto, M. Ichinohe, *Angew. Chem. Int. Ed.* **2003**, *42*, 1143–1145; *Angew. Chem.* **2003**, *115*, 1175–1177.
[40] G. Molev, B. Tumanskii, D. Sheberla, M. Botoshansky, D. Bravo-Zhivotovskii, Y. Apeloig, *J. Am. Chem. Soc.* **2009**, *131*, 11698–11700.
[41] R. Holzner, A. Kaushansky, B. Tumanskii, P. Frisch, F. Linsenmann, S. Inoue, *Eur. J. Inorg. Chem.* **2019**, *2019*, 2977–2981.
[42] W. P. Freeman, T. D. Tilley, F. P. Arnold, A. L. Rheingold, P. K. Gantzel, *Angew. Chem. Int. Ed.* **1995**, *34*, 1887–1890; *Angew. Chem.* **1995**, *107*, 2029–2031.
[43] W. P. Freeman, T. D. Tilley, L. M. Liable-Sands, A. L. Rheingold, *J. Am. Chem. Soc.* **1996**, *118*, 10457–10468.
[44] The bond lengths alternation is quantified by the parameter Δ which is the difference between the lengths of the central C2-C3 bond of the butadiene moiety and the mean value of the C1-C2 and C3-C4 bonds.
[45] J. M. Dysard, T. D. Tilley, *J. Am. Chem. Soc.* **1998**, *120*, 8245–8246.
[46] J. M. Dysard, T. D. Tilley, *J. Am. Chem. Soc.* **2000**, *122*, 3097–3105.
[47] J. M. Dysard, T. D. Tilley, *Organometallics* **2000**, *19*, 4720–4725.
[48] W. P. Freeman, J. M. Dysard, T. D. Tilley, A. L. Rheingold, *Organometallics* **2002**, *21*, 1734–1738.
[49] B. Niepötter, D. Stalke, *Organosilicon Compounds*, Ed.: V. Y. Lee, Academic Press, **2017**, pp. 3–58.
[50] C. Fekete, I. Kovács, L. Nyulászi, T. Holczbauer, *Chem. Commun.* **2017**, *53*, 11064–11067.
[51] V. Y. Lee, R. Kato, M. Ichinohe, A. Sekiguchi, *J. Am. Chem. Soc.* **2005**, *127*, 13142–13143.
[52] H. Yasuda, V. Y. Lee, A. Sekiguchi, *J. Am. Chem. Soc.* **2009**, *131*, 6352–6353.
[53] Z. Dong, M. Schmidtmann, T. Müller, *Chem. Eur. J.* **2019**, *25*, 10858–10865.
[54] Z. Chen, C. S. Wannere, C. Corminboeuf, R. Puchta, P. v. R. Schleyer, *Chem. Rev.* **2005**, *105*, 3842–3888.
[55] A. Stanger, *J. Org. Chem.* **2006**, *71*, 883–893.

Manuscript received: April 20, 2021
Accepted manuscript online: May 12, 2021
Version of record online: June 1, 2021

